Volume 8 | Number 1 | 7 January 2021

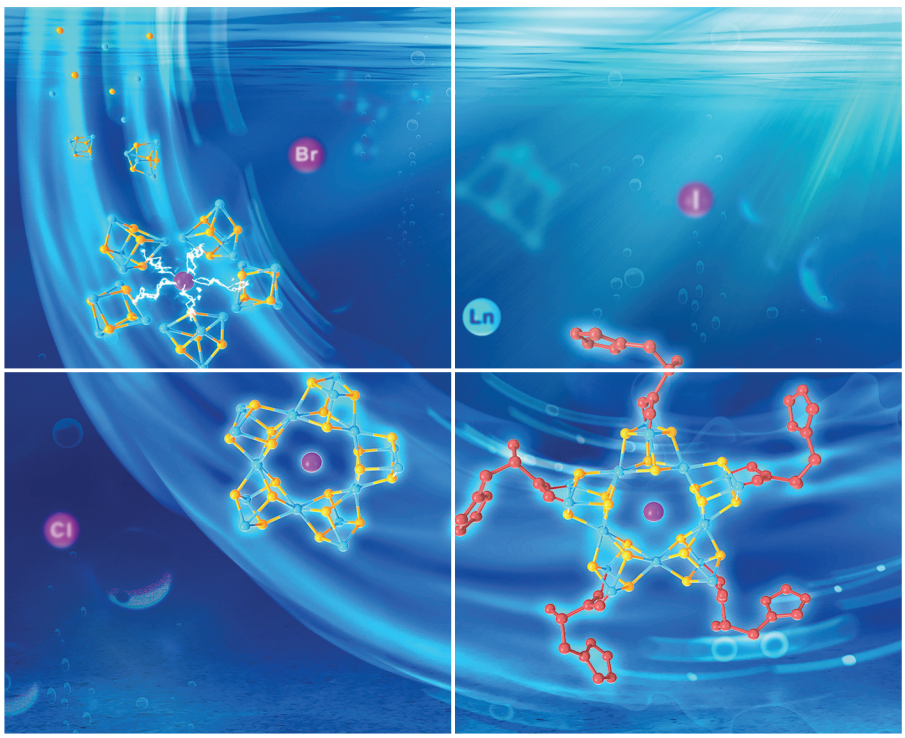

INORGANIC CHEMISTRY

FRONTIERS

CCS 中国化学会 CHINESE CHEMICAL SOCIETY
PEKING UNIVERSITY 1898
ROYAL SOCIETY OF CHEMISTRY
rsc.li/frontiers-inorganic

INORGANIC CHEMISTRY FRONTIERS

RESEARCH ARTICLE

View Article Online
View Journal | View Issue

Cite this: *Inorg. Chem. Front.*, 2021, **8**, 26

A systematic study of halide-template effects in the assembly of lanthanide hydroxide cluster complexes with histidine†‡

Weiming Huang,§[a] Zhonghao Zhang,§[b] Yinglan Wu,§[b] Wanmin Chen,[a] David A. Rotsch,[c] Louis Messerle*[c] and Zhiping Zheng *[a,b]

Received 17th August 2020,
Accepted 29th September 2020

DOI: 10.1039/d0qi01004a

rsc.li/frontiers-inorganic

A series of polynuclear lanthanide (Ln) complexes were prepared by the hydrolysis of lanthanide ions using L-histidine as a supporting ligand. Halide ions (X^- = Cl^-, Br^-, and I^-) have been found to play a major role in templating the assembly of pentadecanuclear complexes for Nd(III) and Gd(III) with the definitive evidence of μ_5-X^- in the cluster core formed by five corner-shared cubane units of $[Ln_4(\mu_3\text{-}OH)_4]^{8+}$. For the heavier and smaller Er(III), analogous pentadecanuclear complex templates by μ_5-Cl^- and μ_5-Br^- were also isolated, but an otherwise identical reaction in the presence of added I^- afforded a dodecanuclear complex with a core of four corner-shared cubanes. Two I^- guests are found, one on each side of the wheel-like structure and in close contact with the μ_3-OH groups. For the medium size Gd(III), a dodecanuclear complex with two I^- can also be formed by changing the metal–ligand ratio. The halide-template effects are analyzed, and the production of different cluster complexes can be rationalized by invoking the match of the physical size of the lanthanide and halide ions. The magnetic properties of dodecanuclear **6** were investigated for magnetic cooling applications, and it showed a magnetic entropy change of 30.95 J kg^{-1} K^{-1} at 2 K for 7 T.

Introduction

Polynuclear lanthanide complexes with cluster-like cores, once synthetic serendipities and prerogatives of academic postulation,[1] have now emerged as an interesting class of compounds with potentially useful applications as highly efficient contrast agents for biomedical imaging,[2,3] molecule-based magnetic materials for information storage and magnetic refrigeration,[4–10] and luminescent probes for structural and functional studies of biological systems.[11–13] Arguably the most extensively studied polynuclear lanthanide complexes are those structurally characterized by a well-defined cluster-type hydroxide core encapsulated by a coordination sphere formed by organic ligands,[14] including β-diketonates,[15–17] α-amino acids,[18–22] and other more specialized ligands.[14,23] Numerous cluster complexes of this kind have appeared in the literature since our report on a pentadecanuclear complex of europium hydroxide using the now commonly adopted synthetic approach of ligand-controlled hydrolysis.[20] The essence of this method is to carry out the hydrolysis of a lanthanide ion in the presence of judiciously chosen ligands, organic or small inorganic coordinating anions (Scheme 1).[20,21,24–28] The otherwise uncontrollable lanthanide hydrolysis is arrested or limited due to the pre-occupation of the metal's coordination sphere by the ancillary ligand(s). The degree of olation reaction is limited, leading to structurally and compositionally well-defined clusters rather than intractable precipitates of lanthanide oxides or hydroxides.[22,29]

The identity of the resulting cluster complexes has been found to be highly dependent on the nature of both the

[a]*Department of Chemistry and Shenzhen Grubbs Institute, Southern University of Science and Technology, Shenzhen 518055, China. E-mail: zhengzp@sustech.edu.cn*
[b]*Department of Chemistry and Biochemistry, The University of Arizona, Tucson, AZ 85721, USA*
[c]*Department of Chemistry, The University of Iowa, Iowa City, IA 52242, USA*
† In memory of Guangxian Xu on the centenary of his birth.
‡ Electronic supplementary information (ESI) available. CCDC 2015727–2015736. For ESI and crystallographic data in CIF or other electronic format see DOI: 10.1039/d0qi01004a
§ These authors contributed equally to this work.

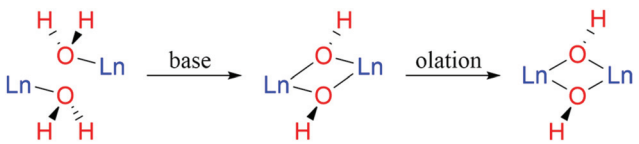

Scheme 1 Ligand-controlled hydrolysis of lanthanide (Ln) ions, affording polynuclear lanthanide oxide/hydroxide complexes with cluster-type core motifs.

lanthanide ion and the ligand, the strength of the base used, and the overall pH condition of the reaction mixture.[16] A great variety of cluster core motifs have been documented in the literature including the diamond-shaped hydroxo-bridged dinuclear motif that resembles the active-site structure of many nucleases.[30] In the course of such studies, anionic species such as halide ions,[31–34] ClO_4^-,[35] CO_3^{2-},[36,37] and NO_3^-[38] have been found to be instrumental for the assembly of many of the clusters, in particular heterometallic ones containing both lanthanide and transition metal elements. The incorporation of such anions is often unintended and unexpected, but examples do exist when certain anions are added on purpose to enhance the synthesis,[20,21] generally after the accidental discovery of the presence of such species in the product.

In our original report[20] and a subsequent full article,[21] the templating role of halide ions for the assembly of a series of lanthanide hydroxide cluster complexes with tyrosinate ligands has been unambiguously established. Specifically, the cluster nuclearity has been found to be critically dependent on the size of the halide template. Pentadecanuclear complexes were obtained with μ_5-Cl^- or μ_5-Br^- serving as the template, whereas in the presence of I^-, dodecanuclear complexes were isolated as the product. The structures of the pentadeca- and dodecanuclear cluster motifs, composed respectively of five and four corner-sharing cubane-like units of $[Ln_4(\mu_3\text{-}OH)_4]^{8+}$, are shown in Fig. 1, together with the clear evidence of the halide template(s).

The assembly of these multi-cubane cluster complexes with tyrosinate ligands was surprising, standing in stark contrast to the production of single-cubane clusters when other α-amino acids were used as hydrolysis-limiting ligands.[19] The case of phenylalanine is most revealing as it differs from tyrosine only in its benzyl side group with respect to the 4-hydroxybenzyl group in the latter. We suspect that for amino acids with a less polar and/or noncoordinating side chain, the point of incipient precipitation of lower-nuclearity clusters, such as single-cubane clusters, is reached prior to any more extensive hydrolysis that may occur. In comparison, a more polar side-chain functional group in an amino acid is expected to enhance the water solubility of the corresponding complex, for which further hydrolysis may be possible, leading to clusters of higher nuclearities. Lending support to this hypothesis is the isolation of cationic cluster complexes $[Gd_{14}(\mu_4\text{-}OH)_2(\mu_3\text{-}OH)_{16}(H_2O)_8(\text{L-serine})_{20}]^{3+}$ and $[Er_{60}(\text{L-threonine})_{34}(\mu_6\text{-}CO_3)_8(\mu_3\text{-}OH)_{96}(\mu_2\text{-}O)_2(H_2O)_{18}]^{30+}$ for which the hydrolysis-limiting ancillary ligands are L-serine and L-threonine, respectively, both bearing hydroxyl groups.[22,39]

In this work, we provide yet another example of using an amino acid with a hydrophilic side-chain group for the assembly of higher-nuclearity lanthanide clusters. Specifically, we report the halide-templated syntheses and structural studies of ten closely related cubane-wheel cluster complexes with L-histidine – an α-amino acid featuring an imidazolyl side group – as a supporting ligand. More importantly, with the use of representative light, medium and heavy lanthanide ions in the systematic studies described herein, we were able to correlate the identity (nuclearity and structure) of the resulting cluster complexes with the size of the halide templates – a significant aspect of templated synthesis that has not been achieved. Furthermore, the magnetic properties of dodecanuclear **6** were studied as Gd(III)-containing clusters are of interest for magnetic cooling applications due to the maximum number (7) of electrons that can be offered by one Gd(III) ion.

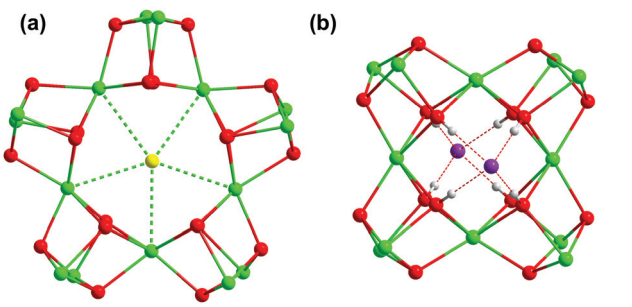

Fig. 1 The core structures of pentadeca- (a) and dodecanuclear (b) lanthanide hydroxide complexes with their respective halide guest(s). Color legends: Ln, green; O, red; Cl^-/Br^-, yellow; I^-, purple; H, gray.

Experimental section

Materials

Chemicals were purchased from a commercial source and were used as received (Table S1‡). Aqueous solutions of $Ln(ClO_4)_3$ (Ln = Nd, Gd, and Er) were prepared by first digesting Ln_2O_3 in 70% perchloric acid, followed by dilution with de-ionized water to 1.0 M. Elemental analyses (C, H, and N) were carried out using a Vario EL III elemental analyzer; samples were dried to constant weight over a desiccant prior to analysis. Infrared (IR) spectra were recorded with a Bruker Alfa spectrophotometer. Magnetic data were obtained with a polycrystalline sample in a sample tube located in a brass cell on a SQUID MPMS3 magnetometer. *Caution*: Perchlorates are potentially explosive and should be handled with great care and in small amounts.

Preparation of compounds

$[Nd_{15}(\mu_5\text{-}Cl)(\mu_3\text{-}OH)_{20}(His)_{10}(H\text{-}His)_5(H_2O)_9]Cl_4(ClO_4)_{10}\cdot 16H_2O$ (1) (note: H-His, histidine; His, monodeprotonated form of histidine). A mixture containing L-histidine (0.310 g, 2.00 mmol), $Nd(ClO_4)_3$ (aq. 1.0 M, 2.0 mL), and NaCl (0.029 g, 0.50 mmol) was stirred with heating at about 80 °C. To this solution was added freshly prepared NaOH (aq. 1.0 M) up to the point of incipient but permanent precipitation. The resulting mixture was then filtered while hot, and the filtrate was allowed to cool naturally in a vial covered with Parafilm. The product was obtained as a violet crystalline solid in 39% yield (based on Nd). Selected IR data (cm^{-1}): 3676(w), 3653(w), 2985(s), 2970(s), 2904(s), 1559(m), 1438(m), 1411(m), 1257(w), 1227(w), 1065(s), 1055(s), 892(w), 682(w), 622(m). Anal. Calcd for $C_{90}H_{195}Cl_{15}Nd_{15}N_{45}O_{115}$ (FW =

6443.14): C, 16.78%; H, 3.05%; N, 9.78%. Found: C, 16.86%; H, 2.74%; N, 9.71%.

$[Nd_{15}(\mu_5\text{-}Br)(\mu_3\text{-}OH)_{20}(His)_{10}(H\text{-}His)_4(H_2O)_{12}]Br_3(ClO_4)_{11}\cdot 9H_2O$ (2). With the use of NaBr (0.051 g, 0.50 mmol) in place of NaCl, **2** was prepared by an otherwise identical procedure as described above for the synthesis of **1**, in 35% yield (based on Nd). Selected IR data (cm^{-1}): 3748(w), 3675(m), 2986(s), 2904(s), 1406(m), 1393(m), 1254(m), 1226(m), 1067(s), 1053(s), 889(w), 624(m). Anal. Calcd for $C_{84}H_{178}Br_4Cl_{11}Nd_{15}N_{42}O_{113}$ (FW = 6457.72): C, 15.62%; H, 2.78%; N, 9.11%. Found: C, 15.63%; H, 2.49%; N, 9.11%.

$[Nd_{15}(\mu_5\text{-}I)_{0.5}(\mu_5\text{-}OH)_{0.5}(\mu_3\text{-}OH)_{20}(His)_{11}(H\text{-}His)_4(H_2O)_9]I(ClO_4)_{12}\cdot 12H_2O$ (3). With the use of NaI (0.075 g, 0.5 mmol) in place of NaCl, **3** was prepared by an otherwise identical procedure for the synthesis of **1**, in 25% yield (based on Nd). Selected IR data (cm^{-1}): 3671(w), 3650(w), 2988(s), 2906(s), 1576(m), 1443(m), 1415(m), 1257(w), 1225(w), 1067(s), 896(w), 672(w), 623(m). Anal. Calcd for $C_{90}H_{186.5}Cl_{12}I_{1.5}Nd_{15}N_{45}O_{119.5}$ (FW = 6869.82): C, 16.40%; H, 2.85%; N, 9.59%. Found: C, 16.39%; H, 2.72%; N, 9.48%.

$[Gd_{15}(\mu_5\text{-}Cl)(\mu_3\text{-}OH)_{20}(His)_{10}(H\text{-}His)_4(H_2O)_8]Cl_6(ClO_4)_8\cdot 22H_2O$ (4). This compound was prepared by adopting the procedure for **1** but using an aqueous solution of $Gd(ClO_4)_3$ in place of $Nd(ClO_4)_3$. The product was obtained as a colorless crystalline solid in 32% yield (based on Gd). Selected IR data (cm^{-1}): 3667(w), 3654(w), 2985(s), 2974(s), 2904(s), 1575(m), 1447(m), 1450(m), 1324(w), 1254(w), 1231(w), 1064(s), 894(w), 703(w), 622(m). Anal. Calcd for $C_{84}H_{196}Cl_{15}Gd_{15}N_{42}O_{110}$ (FW = 6445.21): C, 15.65%; H, 3.07%; N, 9.13%. Found: C, 15.63%; H, 2.62%; N, 9.09%.

$[Gd_{15}(\mu_5\text{-}Br)(\mu_3\text{-}OH)_{20}(His)_{10}(H\text{-}His)_5(H_2O)_6]Br_4(ClO_4)_{10}\cdot 27H_2O$ (5). This compound was prepared by following the procedure for the synthesis of **2** but using an aqueous solution of $Gd(ClO_4)_3$ in place of $Nd(ClO_4)_3$. The product was obtained as a colorless crystalline solid in 16% yield (based on Gd). Selected IR data (cm^{-1}): 3676(w), 3651(w), 2988(s), 2974(s), 2904(s), 1405(m), 1254(w), 1277(w), 1056(s), 894(w), 705(w), 621(m). Anal. Calcd for $C_{90}H_{211}Cl_{10}Br_5Gd_{15}N_{45}O_{123}$ (FW = 7004.66): C, 15.43%; H, 3.04%; N, 9.00%. Found: C, 15.36%; H, 2.50%; N, 9.04%.

$[Gd_{12}I_2(\mu_3\text{-}OH)_{16}(His)_8(H_2O)_{20}](ClO_4)_{10}\cdot 18H_2O$ (6). This compound was prepared by following the procedure for the synthesis of **3** but using an aqueous solution of $Gd(ClO_4)_3$ in place of $Nd(ClO_4)_3$. The product was obtained as a colorless crystalline solid in 47% yield (based on Gd). Selected IR data (cm^{-1}): 3437(br), 2983(w), 2903(w), 1589(s), 1442(s), 1423(s), 1328(m), 1070(s), 825(w), 767(w), 698(m), 680(m), 622(m). Anal. Calcd for $C_{48}H_{156}I_2Cl_{10}Gd_{12}N_{24}O_{110}$ (FW = 5325.18): C, 10.83%; H, 2.95%; N, 6.31%. Found: C, 10.81%; H, 2.53%; N, 6.37%.

$[Gd_{15}(\mu_5\text{-}I)_{0.5}(\mu_5\text{-}OH)_{0.5}(\mu_3\text{-}OH)_{20}(His)_{10}(H\text{-}His)_4(H_2O)_9]I_4(ClO_4)_{10}\cdot 12H_2O$ (7). With a reduced amount of histidine (0.50 mmol *versus* 2.00 mmol for the synthesis of **6**), **7** was obtained in 19% yield (based on histidine) by an otherwise identical procedure for the preparation of **6**. Selected IR data (cm^{-1}): 3399(br), 2989(w), 2909(w), 1587(m), 1442(m), 1422(m), 1333(w), 1060(s), 678(w), 623(m). Anal. Calcd for $C_{84}H_{178.5}Cl_{10}I_{4.5}Nd_{15}N_{42}O_{109.5}$ (FW = 6813.38): C, 14.81%; H, 2.64%; N, 8.63%. Found: C, 14.86%; H, 2.52%; N, 8.58%.

$[Er_{15}(\mu_5\text{-}Cl)(\mu_3\text{-}OH)_{20}(His)_{10}(H\text{-}His)_4(H_2O)_6]Cl_4(ClO_4)_{10}\cdot 20H_2O$ (8). This compound was prepared by following the procedure for the synthesis of **1** but using an aqueous solution of $Er(ClO_4)_3$ in place of $Nd(ClO_4)_3$. The product was obtained as a light-pink crystalline solid in 20% yield (based on Er). Selected IR data (cm^{-1}): 3687(w), 3660(w), 2985(s), 2972(s), 2904(s), 1596(m), 1570(m), 1451(m), 1409(m), 1252(w), 1230(w), 1071(s), 900(w), 792(w), 704(w), 618(m). Anal. Calcd for $C_{84}H_{188}Cl_{15}Er_{15}N_{42}O_{114}$ (FW = 6651.28): C, 15.17%; H, 2.85%; N, 8.84%. Found: C, 15.21%; H, 2.40%; N, 8.78%.

$[Er_{15}(\mu_5\text{-}Br)(\mu_3\text{-}OH)_{20}(His)_{10}(H\text{-}His)_4(H_2O)_6]Br_4(ClO_4)_{10}\cdot 24H_2O$ (9). This compound was prepared by following the synthetic procedure for **2** but using an aqueous solution of $Er(ClO_4)_3$ in place of $Nd(ClO_4)_3$. The product was obtained as a light-pink crystalline solid in 26% yield (based on Er). Selected IR data (cm^{-1}): 3687(w), 3662(w), 2986(s), 2972(s), 2905(s), 1572(m), 1447(m), 1407(m), 1257(w), 1227(w), 1065(s), 800(w), 705(w), 620(w). Anal. Calcd for $C_{84}H_{196}Br_5Cl_{12}Er_{15}N_{42}O_{118}$ (FW = 6945.60): C, 14.53%; H, 2.84%; N, 8.47%. Found: C, 14.51%; H, 2.43%; N, 8.42%.

$[Er_{12}I_2(\mu_3\text{-}OH)_{16}(His)_8(H_2O)_{20}](ClO_4)_{10}\cdot 22H_2O$ (10). This compound was prepared by following the procedure for the synthesis of **3** but using an aqueous solution of $Er(ClO_4)_3$ in place of $Nd(ClO_4)_3$. The product was obtained as a light-pink crystalline solid in 18% yield (based on Er). Selected IR data (cm^{-1}): 3690(w), 3664(w), 2988(s), 2971(s), 2904(s), 1595(w), 1409(m), 1248(m), 1227(m), 1068(s), 1053(s), 891(w), 618(m). Anal. Calcd for $C_{48}H_{164}I_2Cl_{10}Er_{12}N_{24}O_{114}$ (FW = 5409.3): C, 10.45%; H, 3.00%; N, 6.09%. Found: C, 10.52%; H, 2.31%; N, 6.04%.

X-ray crystallography

Crystallographic data for **1–10** were collected on a Bruker APEX-II CCD diffractometer with Mo-Kα radiation (λ = 0.71073 Å) at 100(2) K. Absorption corrections were applied using the multi-scan program SADABS. The structures were solved by the Intrinsic Phasing method (SHELXTL)[40] and using Olex2 as the graphical interface.[41] Disordered water molecules were removed by using the PLATON/SQUEEZE program.[42] Therefore, all formulae were determined based on satisfactory microanalyses (CHN) and charge balancing. The non-hydrogen atoms were refined anisotropically by using the full-matrix least-squares method on F^2. Crystal data and details of the data collection and refinement are presented in the ESI.‡

Results and discussion

Preparation of compounds

Compounds **1–10** (Table 1) were prepared by the hydrolysis of three different lanthanide ions in the presence of L-histidine and with the assistance of a particular halide template.[19–21] This process was promoted by NaOH but controlled by the

Table 1 Nuclearity of **1–10** related to metal ions and templated halide ions

	Metal ions		
Halide ions	Nd^{3+}	Gd^{3+}	Er^{3+}
Cl^-	**1** (Nd_{15})	**4** (Gd_{15})	**8** (Er_{15})
Br^-	**2** (Nd_{15})	**5** (Gd_{15})	**9** (Er_{15})
I^-	**3** (Nd_{15})	**6** (Gd_{12})/**7** (Gd_{15})	**10** (Er_{12})

ancillary and hydrolysis limiting amino acid. All cluster complexes but one were obtained with a metal : histidine molar ratio of 1 : 1, but single crystals of **7** could only be obtained with a 4 : 1 ratio.

Crystal structures

All compounds have been structurally characterized by single-crystal X-ray diffraction studies. Except for some minor differences in the coordination of the histidine ligands, **1–5** and **7–9** share a common wheel-like cluster core composed of five corner-sharing cubane units of $[Ln_4(\mu_3\text{-}OH)_4]^{8+}$ centering around a halide ion; this motif was first reported for analogous cluster complexes supported by the tyrosinate ligand.[20,21]

The side and top views of the structure of **1**, representative of the 8 very similar clusters, are shown in Fig. 2a and b, respectively. The H-His and His ligands occupy two distinct locations with respect to the cluster core – on the two sides of the wheel plane and along its rim. The side-capping His ligands along the wheel rim display exclusively a μ_3:η^1,η^2,η^1,η^1 mode with simultaneous participation of the carboxylato and amino groups as well as the side-chain imidazolyl group in metal coordination (Fig. 2c). In comparison, the coordination of the rim-surface metal atoms is more diverse. Specifically, with the sole exception of **3**, the organic ligands are exclusively zwitterionic histidine (H-His), either monodentate or in the carboxylate-bridging mode (Fig. 2d); there are five bridging H-His ligands for **1** and **5**, but four for **2**, **4**, and **7**. Interestingly, the H-His ligands are in both bridging and monodentate modes, two for each, for **8** and **9** (Fig. S1‡). Complex **3** is unique in that in addition to four bridging

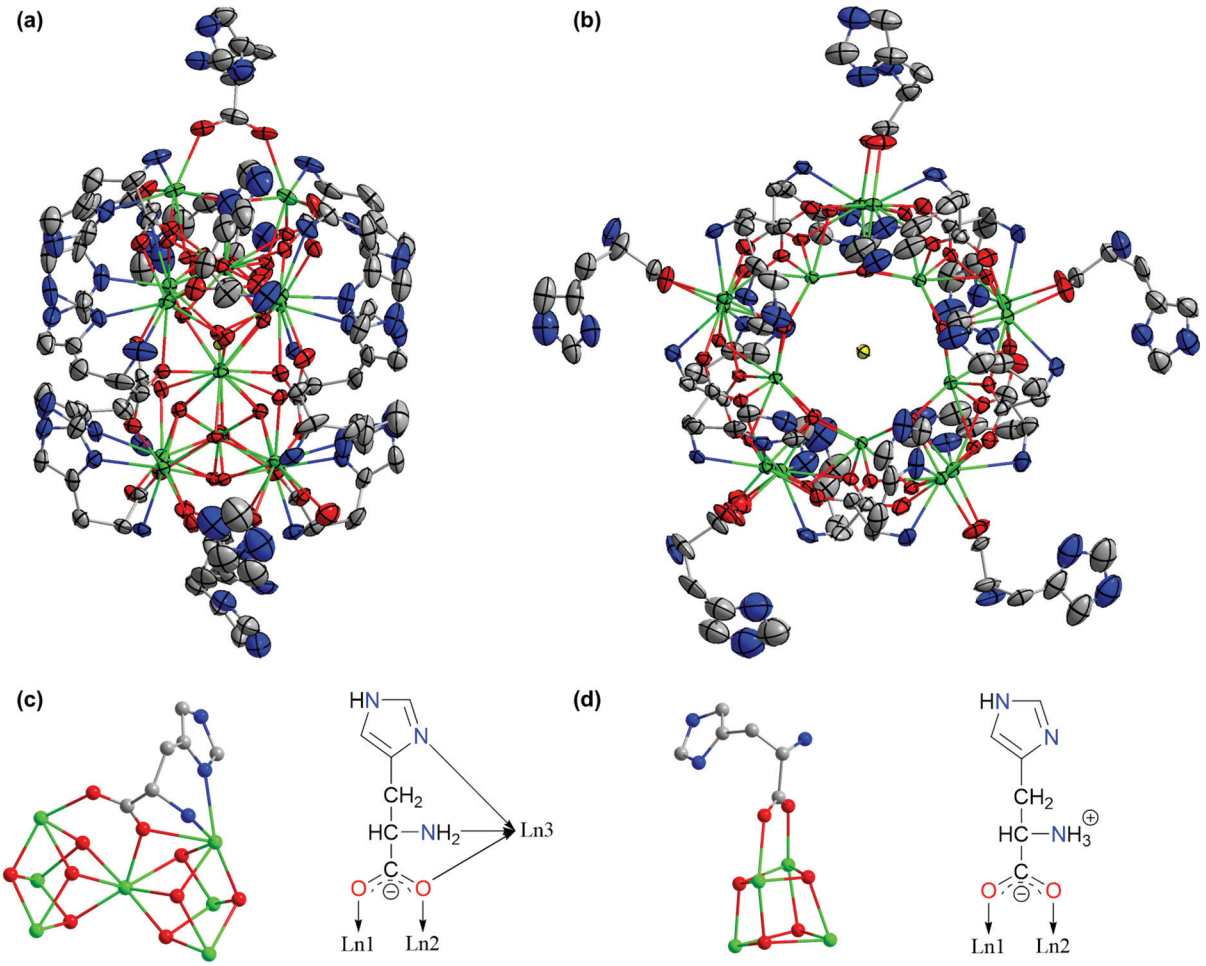

Fig. 2 Crystal structure of cationic pentadecanuclear **1** viewed in the direction of the wheel rim (a) and along the direction of the wheel side (b). A fragment of two corner-shared $[Nd_4(\mu_3\text{-}OH)_4]^{8+}$ units with the evidence of a μ_3:η^1,η^2,η^1,η^1 mode of the side-capping histidine ligand (c) and a cubane unit with the evidence of a bridging mode of the ligands along the outer rim of the cluster wheel (d). Color legends: C, gray; N, blue; O, red; Nd, green; Cl, yellow (H atoms are omitted for clarity).

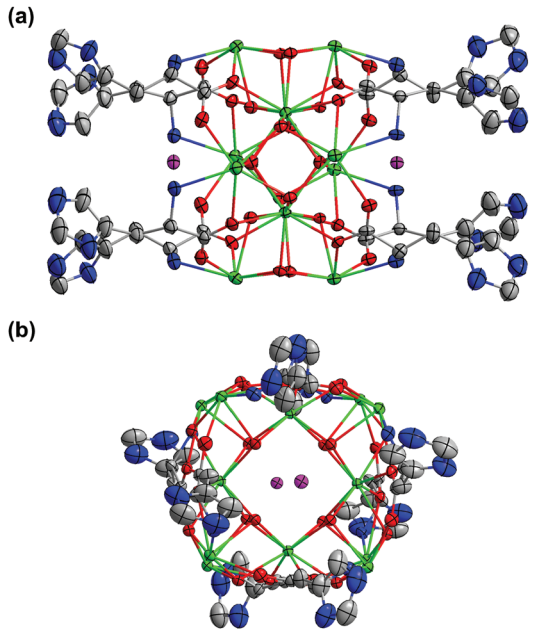

Fig. 3 Crystal structure of cationic dodecanuclear **10** viewed in the direction of the wheel rim (a) and along the direction of the wheel side (b). Color legends: C, grey; N, blue; O, red; Er, green; I, purple (H atoms are omitted for clarity).

ligands, the fifth ligand is actually His, coordinating the rim-surface Gd(III) using its amino group and its carboxylate group in a monodentate fashion (Fig. S2‡).

Complexes **6** and **10** share a common dodecanuclear cluster core motif that consists of four corner-sharing $[Ln_4(\mu_3\text{-}OH)_4]^{8+}$ (Ln = Gd, **6**; Er, **10**) units with two I^- ions, one sitting above and the other below the plane of the cubane-wheel (Fig. 3). There are only eight His ligands, four on each side of the wheel structure and exclusively in a μ_3:η^1,η^2,η^1 mode (Fig. S3‡) that is identical to the one observed previously for the tyrosinate ligand;[20,21] neither His nor H-His ligands are present along the rim of these two complexes.

The metric values of the core parameters of **1–3**, representative of the pentadecanuclear complexes templated by different halide ions and those of **6**, representative of the dodecanuclear complexes are presented in Table S4.‡ The Ln–O and Ln–N bond lengths and the Ln–O–Ln and O–Ln–O angles within the cubane units fall in the corresponding normal ranges reported for similar complexes.[23,43] Crystal data and selected bond distances for all complexes are presented in the ESI.‡

Halide-template effects

The templating role of Cl^- and Br^- ions in the assembly of pentadecanuclear cluster complexes with tyrosinate ligands has previously been established.[20,21] Specifically, with light and medium lanthanide ions, including Pr(III), Nd(III), Eu(III), and Gd(III), only pentadecanuclear cluster complexes featuring μ_5-Cl^- or μ_5-Br^- were obtained, while for two heavier lanthanide ions, Dy(III) and Er(III), only dodecanuclear complexes with two I^- guests were isolated. Intuitively, the right size-fit between a halide ion and the cavity of the cubane-wheel was suspected to be critical in the cluster assembly. However, definitive evidence based on the combination of the same lanthanide ion and all three different-sized halide ions is not available at present. Also lacking is the evidence suggesting the "discrimination" of one specific halide ion, especially the bulky I^- ion, against any particular lanthanide ions in the cluster assembly when their sizes are systematically changed. In this work, we have obtained some of this information by securing three sets of cluster complexes with the use of Nd(III), Gd(III), and Er(III) representing light, medium and heavy lanthanide ions, respectively, under the influence of three different halide ions.

Not surprisingly, pentadecanuclear clusters templated by μ_5-Cl^- (**1**), μ_5-Br^- (**2**), and μ_5-I^- (**3**) were obtained with the lightest and largest Nd(III) of the three lanthanides studied. As these three clusters differ only in the size of the halide ions, the nature of the cluster can be unambiguously correlated with the bulk of the template; the average distances between different halide ions and the Nd(III) ions shared at the cubane corner are 3.312, 3.339, and 3.392 Å for Cl^-, Br^-, and I^-, respectively, all being longer than the respective sum of the van der Waals radii of Nd(III) and the halide ion. As such, the halide ion can readily fit into the cavity of the wheel (entries 1–3, Table 2).[44,45] Even so, the space-filling models (Fig. 4) do reveal recognizable albeit subtle differences in the spacing between the halide template and the surrounding O and Nd atoms. Note that **3** and **7** are the first and only known examples of I-templated cubane wheels in this series of clusters; this rarity is a reflection of the small difference between

Table 2 Comparison between the Ln–X distance and van der Waals radii of Nd^{3+} (1.12 Å), Gd^{3+} (1.06 Å), Er^{3+} (1.00 Å), Cl^- (1.81 Å), Br^- (1.96 Å), and I^- (2.20 Å) for all pentadecanuclear **1–5** and **7–9**

Complex	Average Ln–X distance (Å)	Species of metal ion	$r(Ln^{3+})$ (Å)	Species of halide ion	$r(X^-)$ (Å)	$r(Ln^{3+}) + r(X^-)$	The difference between column 2 and column 7
1	3.31	Nd^{3+}	1.12	Cl^-	1.81	2.93	+0.38
2	3.34	Nd^{3+}	1.12	Br^-	1.96	3.08	+0.26
3	3.39	Nd^{3+}	1.12	I^-	2.20	3.32	**+0.07**
4	3.23	Gd^{3+}	1.06	Cl^-	1.81	2.87	+0.36
5	3.26	Gd^{3+}	1.06	Br^-	1.96	3.02	+0.24
7	3.27	Gd^{3+}	1.06	I^-	2.20	3.26	**+0.01**
8	3.17	Er^{3+}	1.00	Cl^-	1.81	2.81	+0.36
9	3.19	Er^{3+}	1.00	Br^-	1.96	2.96	+0.23

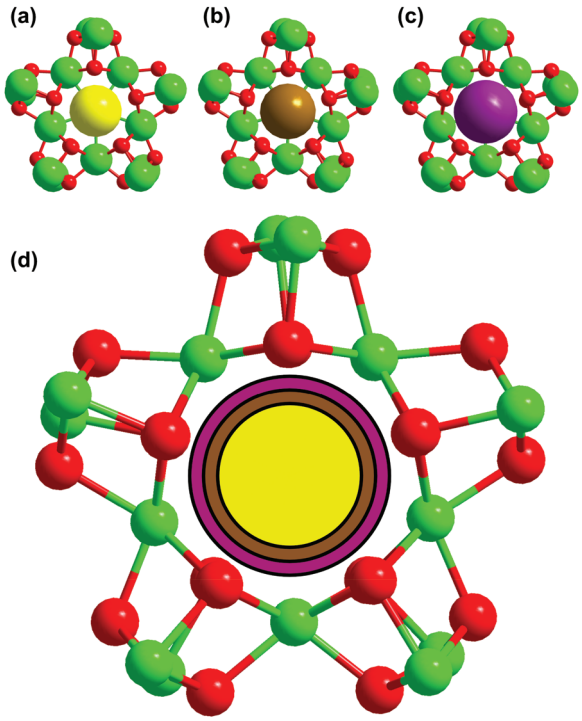

Fig. 4 Space-filling models of **1** (a), **2** (b), and **3** (c), constructed using the precise van der Waals radii of Nd^{3+} (1.12 Å), Cl^- (1.81 Å), Br^- (1.96 Å), and I^- (2.20 Å). Illustration of different halide anions fit into the pentagonal cavity. Color legends: O, red; Nd, green; Cl, yellow; Br, brown; I, purple.

the Ln–I (Ln = Nd, Gd) distance and the sum of the corresponding van der Waals radii (entries 3 and 7, Table 2).

For the sizably smaller Er(III), although pentadecanuclear clusters **8** and **9** (entries 7 and 8, Table 2) with the respective Cl^- and Br^- templates were obtained, their I^--templated cognate has so far eluded us despite our repeated attempts. Instead, the dodecanuclear cluster **10** was obtained with the incorporation of two I^- ions (Fig. 3). Nevertheless, the absence of an I^--templated cluster of Er(III) is not entirely surprising as the difference between the average Ln–I distance and the sum of the corresponding van der Waals radii decreases from 0.07 Å for Nd(III) to 0.01 Å for Gd(III); following this trend, a pentagonal cavity formed by the noticeably smaller Er(III) is probably not large enough for the encapsulation of the bulky I^- ion. It needs to be emphasized that although the formation of templated clusters may be understood or "rationalized" in terms of the ability of a "preformed" cluster wheel for the subsequent accommodation of the halide guest, it is the anion that serves as a kinetic template in the assembly of the wheel-like cluster complex because, in the absence of a halide ion, hexanuclear hydroxide clusters with an interstitial μ_6-O^{2-} can be isolated.[46,47]

The assembly of the I^--containing dodecanuclear complexes remains to be rationalized. Previously, a template-free dodecanuclear complex with the same cluster core was isolated when ethylenediamine tetraacetic acid (EDTA) was used as the hydrolysis-limiting ligand.[29] The presence of another template-free tetra-cubane motif, though not standalone, has also been recognized in the 24-cubane cage-like Ln_{60} cluster complexes with threonine.[22] These literature precedents suggest that the operation of a template is not essential for the assembly of the tetra-cubane clusters. In the present dodecanuclear **6** and **10**, the average distance between the iodide ion and the oxygen atoms of the μ_3-OH groups is 3.605 Å. This distance is almost the same as the sum of the van der Waals radii of I^- (2.20 Å) and OH^- (1.35 Å),[44,45] indicating a very compact arrangement with the I^- ion snuggling on top of the square formed by four μ_3-OH groups. Thus, the I^- ions should be more appropriately termed as "guests" that are incorporated due to the electrostatic interactions by the μ_3-OH groups following the formation of the template-free cluster wheel rather than authentic templates.

If the above arguments hold, then for a medium lanthanide ion such as Gd(III) in this work, the formation of both the pentadeca- and dodecanuclear clusters may be possible as the medium-sized metal ion serves as the transitioning point between the larger/lighter Nd(III) and the smaller/heavier Er(III) ion. But this dual possibility also creates a dilemma, that is, the reaction may be experiencing some kind of frustration as both pathways are possible, and in fact with little difference energetically considering the primarily ionic lanthanide–ligand interactions. This conjecture is corroborated by the challenges we encountered in securing dodecanuclear **6** and pentadecanuclear **7**. Only by adjusting the Gd–histidine ratio and after multiple painstaking attempts were we able to obtain the desired cluster targets. But the reason why the change of this particular parameter was successful remains unclear.

Magnetic properties

Recent interest in high-nuclearity lanthanide-containing clusters lies primarily in their possible applications for magnetic cooling – a cooling technology that is energy efficient and environmentally friendly.[48] Of particular interest are clusters containing Gd(III) ions as each Gd(III) can offer 7 unpaired electrons, which is the most for any metal ions. This potential is evaluated by a substance's magnetocaloric effect (MCE), that is, its heating and cooling upon changes in an external magnetic field. Experimentally, MCE is assessed by the magnitude of magnetic entropy change (ΔS_m), calculated by using the Maxwell equation $-\Delta S_m(T) = \int [\partial M(T,H)/\partial T]_H dH$ using the experimentally obtained magnetization data (T, temperature; M, magnetization; H, external magnetic field applied). In this study, the temperature-dependent magnetization of the dodecanuclear Gd(III) cluster **6** was studied in the range of 2 to 300 K with an applied direct-current (dc) magnetic field of 1000 Oe (Fig. 5). The $\chi_M T$ value reached 94.12 cm^3 K mol^{-1} at room temperature, almost the same as the theoretical value of 94.5 cm^3 K mol^{-1} calculated for 12 uncoupled Gd^{3+} ions ($S = 7/2$ and $g = 2$). The $\chi_M T$ value decreases slightly between 50 and 300 K and then rapidly to the minimum value of 49.35 cm^3 K mol^{-1} at 2 K, typical of antiferromagnetic interactions. The χ_m^{-1} *vs.* T plot in the range of 2 to 300 K is shown in Fig. S4,‡

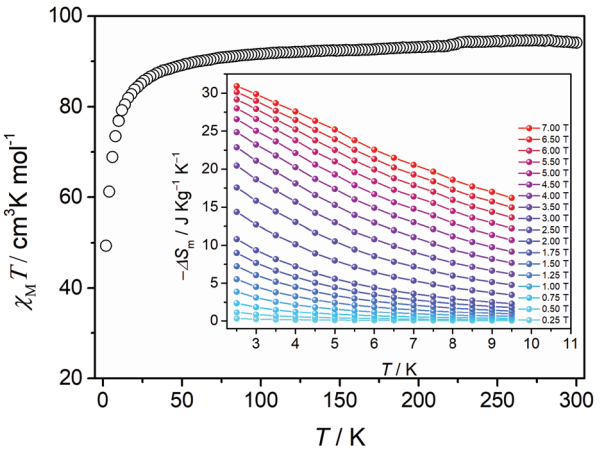

Fig. 5 Plot of temperature dependence of $\chi_M T$ of **6** under a 1000 Oe dc field. Inset: $-\Delta S_m$ calculated by using the magnetization data at various fields (0–7 T) and temperatures (2.5–9.5 K).

and fitting of the data using the Curie–Weiss law produced a Curie constant C = 95.42 cm^3 K mol^{-1} and a Weiss temperature T = −3.84 K, suggesting the presence of antiferromagnetic interactions.[49] Alternating-current susceptibility measurements revealed no frequency-independent behavior in **6** (Fig. S5‡). The molar magnetization $M(H)$ of **6** was measured in the range of 2 to 10 K and 0 to 7 T field range (Fig. S6‡). The maximum magnetization value of 81.66 $N\mu_B$ (where N is the Avogadro constant and μ_B is the Bohr magneton) at 2.5 K and 7 T is slightly smaller than the expected saturation value 84 $N\mu_B$, in agreement with the above Curie–Weiss fitting result.

The entropy change of **6** at different fields and temperatures is presented in Fig. 5 (inset), with a maximum experimental value of 30.95 J kg^{-1} K^{-1} at 2 K and 7 T. This value is sizably smaller than 37.60 J kg^{-1} K^{-1} calculated for 12 uncorrelated Gd^{3+} by using the equation $\Delta S_m = nR\ln(2S + 1) = 12R\ln(8) = 24.95\ R$ (Gd^{3+}: S = 7/2), which can be attributed to the aforementioned intracluster antiferromagnetic interactions.[48] This value places **6** in a comparable position with other Gd(III)-exclusive clusters.[37]

Conclusions

By controlled hydrolysis of lanthanide ions in the presence of supporting histidine ligands, pentadecanuclear and dodecanuclear complexes featuring cluster-type lanthanide hydroxide core motifs composed respectively of five and four corner-sharing cubane units of $[Ln_4(\mu_3\text{-}OH)_4]^{8+}$ were produced. The combination of the lanthanide ion and the added halides is critically important in determining the outcome of the reaction conducted under otherwise identical conditions. Together with the results from our previous work using tyrosine as a hydrolysis-limiting ligand, the templating role played by halide ions leads to the following conclusions:

1. Amino acids are a unique class of supporting ligands for the controlled hydrolysis of lanthanide ions, with polynuclear complexes characterized by well-defined cluster-type hydroxide core motifs being the usual products.

2. With amino acids bearing polar side groups (serine, tyrosine, histidine, and threonine), the controlled hydrolysis favors the assembly of higher-nuclearity clusters. In contrast, cluster complexes cored with a single cubane unit of $[Ln_4(\mu_3\text{-}OH)_4]^{8+}$ are generally obtained with other amino acid ligands. This observation may be rationalized in terms of the enhanced water solubility of the lanthanide-hydroxo intermediates on the way to the ultimate cluster products.

3. In addition to the nature of the amino acid ligands, the nuclearity and specific structure of the multi-cubane clusters, on the basis of current data, appear to be dependent on the lanthanide and the added halide ions, and more specifically, their relative size or bulk. It has been found that lighter and larger lanthanide ions favour the formation of pentadecanuclear complexes whose assembly is templated by all three halide ions. For heavier and smaller lanthanide ions, in the absence of a powerful template such as Cl^- or Br^-, dodecanuclear complexes can be formed, and if available, I^- ions can be incorporated as guests.

4. Interestingly for medium lanthanide ions, the formation of different-nuclearity clusters may be possible, depending merely on the reaction conditions – the lanthanide–histidine ratio in the present work.

5. High-nuclearity lanthanide clusters, whose assembly is templated by a suitable halide template, are of interest as magnetic coolant molecules. As a representative, the magnetic properties of dodecanuclear **6** were investigated.

Conflicts of interest

There are no conflicts to declare.

Acknowledgements

This work was supported by the National Natural Science Foundation of China (no. 21971106), the Shenzhen Nobel Prize Scientists Laboratory Project (C17783101), the Stable Support Project of Key Research Plan of Shenzhen, and start-up fund from SUSTech. The crystallographic assistance on the first batch of crystals by Dr. S. Roberts, G. Hall, G. S. Nichol, and P. Wei is gratefully acknowledged.

Notes and references

1 R. Anwander, "Self-assembly" in organolanthanide chemistry: formation of rings and clusters, *Angew. Chem., Int. Ed.*, 1998, **37**, 599–602.
2 J. Estelrich, M. J. Sánchez-Martín and M. A. Busquets, Nanoparticles in magnetic resonance imaging: from simple to dual contrast agents, *Int. J. Nanomed.*, 2015, **10**, 1727–1741.

3 S. Biju and T. N. Parac-Vogt, Recent advances in lanthanide based nano-architectures as probes for ultra high-field magnetic resonance imaging, *Curr. Med. Chem.*, 2020, **27**, 352–361.
4 P.-B. Jin, Y.-Q. Zhai, K.-X. Yu, R. E. P. Winpenny and Y.-Z. Zheng, Dysprosiacarboranes as organometallic single-molecule magnets, *Angew. Chem., Int. Ed.*, 2020, **59**, 9350–9354.
5 T. Han, Y.-S. Ding and Y.-Z. Zheng, Lanthanide clusters toward single-molecule magnets, in *Recent development in clusters of rare earths and actinides: chemistry and materials*, 2017, vol. 173, pp. 209–314.
6 H.-J. Lun, X.-J. Kong, L.-S. Long and L.-S. Zheng, Trigonal bipyramidal $Co^{III}_2Dy_3$ cluster exhibiting single-molecule magnet behavior, *Dalton Trans.*, 2020, **49**, 2421–2425.
7 X.-Y. Zheng, X.-J. Kong, Z. Zheng, L.-S. Long and L.-S. Zheng, High-nuclearity lanthanide-containing clusters as potential molecular magnetic coolers, *Acc. Chem. Res.*, 2018, **51**, 517–525.
8 Y.-C. Chen, J.-L. Liu and M.-L. Tong, 4f-Clusters for cryogenic magnetic cooling, in *Recent Development in Clusters of Rare Earths and Actinides: Chemistry and Materials*, 2017, vol. 173, pp. 189–207.
9 C.-H. Cui, W.-W. Ju, X.-M. Luo, Q.-F. Lin, J.-P. Cao and Y. Xu, A series of lanthanide compounds constructed from Ln_8 rings exhibiting large magnetocaloric effect and interesting luminescence, *Inorg. Chem.*, 2018, **57**, 8608–8614.
10 W.-P. Chen, P.-Q. Liao, P.-B. Jin, L. Zhang, B.-K. Ling, S.-C. Wang, Y.-T. Chan, X.-M. Chen and Y.-Z. Zheng, The gigantic $\{Ni_{36}Gd_{102}\}$ hexagon: a sulfate-templated "star-of-david" for photocatalytic CO_2 reduction and magnetic cooling, *J. Am. Chem. Soc.*, 2020, **142**, 4663–4670.
11 Z. Ji, Y. Cheng, X. Cui, H. Lin, J. Xu and Y. Wang, Heating-induced abnormal increase in Yb^{3+} excited state lifetime and its potential application in lifetime luminescence nanothermometry, *Inorg. Chem. Front.*, 2019, **6**, 110–116.
12 A. J. Amoroso and S. J. Pope, Using lanthanide ions in molecular bioimaging, *Chem. Soc. Rev.*, 2015, **44**, 4723–4742.
13 K. Y. Zhang, Q. Yu, H. Wei, S. Liu, Q. Zhao and W. Huang, Long-lived emissive probes for time-resolved photoluminescence bioimaging and biosensing, *Chem. Rev.*, 2018, **118**, 1770–1839.
14 X.-Y. Zheng, J. Xie, X.-J. Kong, L.-S. Long and L.-S. Zheng, Recent advances in the assembly of high-nuclearity lanthanide clusters, *Coord. Chem. Rev.*, 2019, **378**, 222–236.
15 C. R. De Silva, F. Li, C. Huang and Z. Zheng, Europium β-diketonates for red-emitting electroluminescent devices, *Thin Solid Films*, 2008, **517**, 957–962.
16 Y. Wu, S. Morton, X. Kong, G. S. Nichol and Z. Zheng, Hydrolytic synthesis and structural characterization of lanthanide-acetylacetonato/hydroxo cluster complexes-a systematic study, *Dalton Trans.*, 2011, **40**, 1041–1046.
17 D. T. Thielemann, I. Fernandez and P. W. Roesky, New amino acid ligated yttrium hydroxy clusters, *Dalton Trans.*, 2010, **39**, 6661–6666.
18 X.-L. Tang, W.-H. Wang, W. Dou, J. Jiang, W.-S. Liu, W.-W. Qin, G.-L. Zhang, H.-R. Zhang, K.-B. Yu and L.-M. Zheng, Olive-shaped chiral supramolecules: simultaneous self-assembly of heptameric lanthanum clusters and carbon dioxide fixation, *Angew. Chem., Int. Ed.*, 2009, **48**, 3499–3502.
19 R. Wang, H. Liu, M. D. Carducci, T. Jin, C. Zheng and Z. Zheng, Lanthanide coordination with α-amino acids under near physiological pH conditions: polymetallic complexes containing the cubane-like $[Ln_4(\mu_3\text{-}OH)_4]^{8+}$ cluster core, *Inorg. Chem.*, 2001, **40**, 2743–2750.
20 R. Wang, Z. Zheng, T. Jin and R. J. Staples, Coordination chemistry of lanthanides at "high" pH: synthesis and structure of the pentadecanuclear complex of europium(III) with tyrosine, *Angew. Chem., Int. Ed.*, 1999, **38**, 1813–1815.
21 R. Wang, H. D. Selby, H. Liu, M. D. Carducci, T. Jin, Z. Zheng, J. W. Anthis and R. J. Staples, Halide-templated assembly of polynuclear lanthanide-hydroxo complexes, *Inorg. Chem.*, 2002, **41**, 278–286.
22 X.-J. Kong, Y. Wu, L.-S. Long, L.-S. Zheng and Z. Zheng, A chiral 60-metal sodalite cage featuring 24 vertex-sharing $[Er_4(\mu_3\text{-}OH)_4]$ cubanes, *J. Am. Chem. Soc.*, 2009, **131**, 6918–6919.
23 L. Qin, G.-J. Zhou, Y.-Z. Yu, H. Nojiri, C. Schroder, R. E. P. Winpenny and Y.-Z. Zheng, Topological self-assembly of highly symmetric lanthanide clusters: a magnetic study of exchange-coupling "fingerprints" in giant Gadolinium(III) Cages, *J. Am. Chem. Soc.*, 2017, **139**, 16405–16411.
24 D. A. Rotsch, D. C. Swenson and L. Messerle, *Halide-templated and halide-free polylanthanide(*III, *) α-amino acid complexes. 238th National Meeting*, American Chemical Society, Washington, DC, 2009.
25 D. A. Rotsch, D. C. Swenson and L. Messerle, *Synthetic, structural, and physicochemical studies on anion-templated polyeuropium(III) complexes of α-amino acids. 237th National Meeting*, American Chemical Society, Sci Mix poster session, Salt Lake City, UT, USA, 2009.
26 D. A. Rotsch, *Hydroxyl-bridged lanthanide amino acid clusters and hexatantalum and hexatungsten chloride clusters: synthesis, characterization, and relevance to biomedical imaging*, PhD thesis, The University of Iowa, Iowa City, IA, USA, 2011.
27 X.-Y. Zheng, Y.-H. Jiang, G.-L. Zhuang, D.-P. Liu, H.-G. Liao, X.-J. Kong, L.-S. Long and L.-S. Zheng, A gigantic molecular wheel of $\{Gd_{140}\}$: a new member of the molecular wheel family, *J. Am. Chem. Soc.*, 2017, **139**, 18178–18181.
28 X.-Y. Zheng, J.-B. Peng, X.-J. Kong, L.-S. Long and L.-S. Zheng, Mixed-anion templated cage-like lanthanide clusters: Gd_{27} and Dy_{27}, *Inorg. Chem. Front.*, 2016, **3**, 320–325.
29 Z. Zheng, Ligand-controlled self-assembly of polynuclear lanthanide-oxo/hydroxo complexes: from synthetic serendipity to rational supramolecular design, *Chem. Commun.*, 2001, **24**, 2521–2529.
30 S. J. Franklin, Lanthanide-mediated DNA hydrolysis, *Curr. Opin. Chem. Biol.*, 2001, **5**, 201–208.

31 N.-F. Li, Q.-F. Lin, X.-M. Luo, J.-P. Cao and Y. Xu, Cl^{-}-templated assembly of novel peanut-like $Ln_{40}Ni_{44}$ heterometallic clusters exhibiting a large magnetocaloric effect, *Inorg. Chem.*, 2019, **58**, 10883–10889.
32 Y.-L. Miao, J.-L. Liu, J.-D. Leng, Z.-J. Lin and M.-L. Tong, Chloride templated formation of $\{Dy_{12}(OH)_{16}\}^{20+}$ cluster core incorporating 1,10-phenanthroline-2,9-dicarboxylate, *CrystEngComm*, 2011, **13**, 3345–3348.
33 J.-J. Yin, C. Chen, G.-L. Zhuang, J. Zheng, X.-Y. Zheng and X.-J. Kong, Anion-dependent assembly of 3d-4f heterometallic clusters Ln_5Cr_2 and Ln_8Cr_4, *Inorg. Chem.*, 2020, **59**, 1959–1966.
34 X.-Y. Li, H.-F. Su, Q.-W. Li, R. Feng, H.-Y. Bai, H.-Y. Chen, J. Xu and X.-H. Bu, A giant Dy_{76} cluster: a fused bi-nanopillar structural model for lanthanide clusters, *Angew. Chem., Int. Ed.*, 2019, **58**, 10184–10188.
35 F.-S. Guo, Y.-C. Chen, L.-L. Mao, W.-Q. Lin, J.-D. Leng, R. Tarasenko, M. Orendáč, J. Prokleška, V. Sechovský and M.-L. Tong, Anion-templated assembly and magnetocaloric properties of a nanoscale $\{Gd_{38}\}$ cage versus a $\{Gd_{48}\}$ barrel, *Chem. – Eur. J.*, 2013, **19**, 14876–14885.
36 J. Cai, X.-Y. Zheng, J. Xie, Z.-H. Yan, X.-J. Kong, Y.-P. Ren, L.-S. Long and L.-S. Zheng, Anion-dependent assembly of heterometallic 3d–4f clusters based on a lacunary polyoxometalate, *Inorg. Chem.*, 2017, **56**, 8439–8445.
37 X.-M. Luo, Z.-B. Hu, Q.-F. Lin, W. Cheng, J.-P. Cao, C.-H. Cui, H. Mei, Y. Song and Y. Xu, Exploring the performance improvement of magnetocaloric effect based Gd-exclusive cluster Gd_{60}, *J. Am. Chem. Soc.*, 2018, **140**, 11219–11222.
38 X.-J. Kong, Y.-P. Ren, L.-S. Long, Z. Zheng, G. Nichol, R.-B. Huang and L.-S. Zheng, Dual shell-like magnetic clusters containing Ni^{II} and Ln^{III} (Ln = La, Pr, and Nd) ions, *Inorg. Chem.*, 2008, **47**, 2728–2739.
39 L. Messerle, D. Nolting, L. Bolinger, A. H. Stolpen, B. F. Mullan, D. Swenson and M. Madsen, Transition metal cluster and polygadolinium compounds as a new paradigm for high attenuation and/or relaxivity in contrast media design: crashing the molecular r1 = 100 barrier, *Acad. Radiol.*, 2005, **12**, S46–S47.
40 *SHELXTL (version 5.0), Reference Manual, Siemens Industrial Automation, Analytical Instruments*, Madison, WI, 1995.
41 O. V. Dolomanov, L. J. Bourhis, R. J. Gildea, J. A. K. Howard and H. Puschmann, OLEX2: a complete structure solution, refinement and analysis program, *J. Appl. Crystallogr.*, 2009, **42**, 339–341.
42 A. L. Spek, Single-crystal structure validation with the program PLATON, *J. Appl. Crystallogr.*, 2003, **36**, 7–13.
43 X.-M. Luo, N.-F. Li, Q.-F. Lin, J.-P. Cao, P. Yuan and Y. Xu, A single-ligand-protected $Eu_{60-n}Gd(Tb)_n$ cluster: a reasonable new approach to expand lanthanide aggregations, *Inorg. Chem. Front.*, 2020, **7**, 2072–2079.
44 R. D. Shannon and C. T. Prewitt, Effective ionic radii in oxides and fluorides, *Acta Crystallogr., Sect. B: Struct. Crystallogr. Cryst. Chem.*, 1969, **25**, 925–946.
45 R. D. Shannon, Revised effective ionic radii and systematic studies of interatomic distances in halides and chalcogenides, *Acta Crystallogr., Sect. A: Cryst. Phys., Diffr., Theor. Gen. Crystallogr.*, 1976, **32**, 751–767.
46 D.-S. Zhang, B.-Q. Ma, T.-Z. Jin, S. Gao, C.-H. Yan and T. C. W. Mak, Oxo-centered regular octahedral lanthanide clusters, *New J. Chem.*, 2000, **24**, 61–62.
47 R. Wang, M. D. Carducci and Z. Zheng, Direct hydrolytic route to molecular oxo-hydroxo lanthanide clusters, *Inorg. Chem.*, 2000, **39**, 1836–1837.
48 Y.-Z. Zheng, G.-J. Zhou, Z. Zheng and R. E. P. Winpenny, Molecule-based magnetic coolers, *Chem. Soc. Rev.*, 2014, **43**, 1462–1475.
49 X.-J. Kong, Y.-P. Ren, W.-X. Chen, L.-S. Long, Z.-P. Zheng, R.-B. Huang and L.-S. Zheng, A four-shell, nesting doll-like 3d–4f cluster containing 108 metal ions, *Angew. Chem., Int. Ed.*, 2008, **47**, 2398–2401.

